COMMUNICATION

Check for updates

Ferri- and ferro-magnetism in CaMnMReO6 double double perovskites of late transition metals M = Co and Ni†‡

Elena Solana-Madruga, [ID] [a] Yu Sun, [a] Ángel M. Arévalo-López [ID] [b] and J. Paul Attfield [ID] *[a]

Two new double double perovskites of ideal compositions CaMn-MReO6 (M = Co, Ni) are reported. The M = Co material has refined composition CaMn$_{0.7}$Co$_{1.3}$ReO$_6$ and orders ferrimagnetically below T$_C$ = 188 K with a relatively large saturated magnetisation of 4.5 μ_B. The M = Ni product, CaMn$_{1.2}$Ni$_{0.8}$ReO$_6$, is a remarkable example of a ferromagnetic oxide with four distinct spin sublattices all collinearly ordered below T$_C$ = 152 K.

The versatility of the perovskite structure[1–5] has led to the synthesis and study of many perovskite materials exhibiting a wide range of useful properties. 1 : 1 ordering of cations at the A and B site cations in the basic ABO$_3$ perovskite structure in layered, columnar or rock-salt arrangements[6] leads to AA′B$_2$O$_6$[7,8] or A$_2$BB′O$_6$[9] double perovskites (DPv) but combinations of cation order in both sublattices are uncommon. These double double (or doubly ordered) perovskites usually combine layered and rock-salt motifs of A and B cations respectively.[10–13] A new double double perovskite (DDPv) type was recently reported to combine a columnar arrangement of A-site cations with the rock-salt order of B and B′ cations for RMnMnSbO$_6$ (R = rare earth).[14,15] This structure crystallizes with the tetragonal P4$_2$/n space group and has five independent cation sites according to the composition AA′$_{0.5}$A″$_{0.5}$BB′O$_6$; A (Wyckoff position 4e), A′ (2a) and A″ (2b) sites with ten-fold, tetrahedral and square planar coordinations, respectively, and octahedral sites for B (4c) and B′ (4d) cations. CaMnMReO$_6$ double double perovskites with the same structure were subsequently reported for M = Mn and Fe. These are found to have different charge distributions and magnetic properties, as CaMnFe^{3+}Re^{5+}O$_6$ is ferrimagnetic with Curie temperature T$_C$ = 500 K, while

CaMnMn^{2+}Re^{6+}O$_6$ has a mix of ferro- and antiferro-magnetic spin sublattices ordered below 120 K.[16] To discover the cation and charge distributions for late first row transition metal ions, which have not previously been incorporated into double double perovskites, we report here the syntheses, structure and properties of CaMnMReO$_6$ double double perovskites with M = Co and Ni, which are discovered to have ferromagnetic order over 3 or 4 spin sublattices.

Samples of ideal composition CaMnCoReO$_6$ and CaMnNiReO$_6$ have been treated under high pressure and high temperature conditions using a Walker-type multi anvil apparatus. A stoichiometric mixture of CaMnO$_3$ (obtained by heating a pellet of CaCO$_3$ and MnO in 1 : 1 ratio at 1473 K for 24 h under an O$_2$ flow with intermediate grinding and repelletising), ReO$_2$ and MO (M = Co, Ni) oxides, were packed in a Pt capsule and treated at 10 GPa and 1373 K (for M = Co) or 1473 K (M = Ni) during 20 minutes. The samples were quenched and slowly depressurized to ambient conditions. These synthesis temperatures were found to be optimal for production of the DDPv type phases, as syntheses at 1423–1473 K for M = Co lead to secondary Re phases, while products made at 1373–1423 K for M = Ni contained unreacted ReO$_2$ and NiO. However secondary phases were present for both materials and were not eliminated in repeated syntheses. Laboratory X-ray powder diffraction (XPD) patterns were collected using a D2 Bruker diffractometer. Magnetic susceptibilities (ZFC-FC under an applied magnetic field of 1000 Oe) and magnetization-field loops up to 7 T were measured using an MPMS SQUID magnetometer. Neutron powder diffraction (NPD) patterns collected at room temperature and 1.5 K on the WISH beamline at the ISIS facility were used to determine crystal and magnetic structures.

Fits to XPD (Fig. S1, ESI‡) and NPD data showed that both CaMnMReO$_6$ (M = Co, Ni) samples adopt the P4$_2$/n DDPv structure. XPD patterns reveal traces of secondary ReO$_2$ (1.7 and 3.0 weight% respectively for M = Co, Ni). The NPD patterns (Fig. 1 and ESI‡) show the presence of a rocksalt type monoxide impurity (8.0 and 17.1% respectively for M = Co, Ni). In both cases the cation distribution in the latter refined to composition M$_{0.67}$Mn$_{0.33}$O,

^{a} *Centre for Science at Extreme Conditions (CSEC) and School of Chemistry,*
The University of Edinburgh, EH9 3FD, UK. E-mail: j.p.attfield@ed.ac.uk

^{b} *Univ. Lille, CNRS, Centrale Lille, ENSCL, Univ. Artois, UMR 8181 – UCCS – Unité*
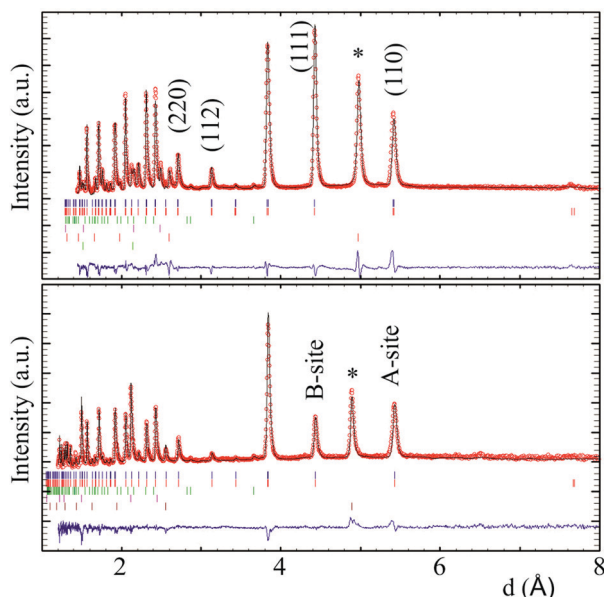*de Catalyse et Chimie du Solide, F-59000 Lille, France*

Fig. 1 Rietveld fits of NPD patterns collected at 1.5 K for CaMnCoReO$_6$ (top) and CaMnNiReO$_6$ (bottom). Bragg markers from top to bottom are the nuclear and magnetic structures of the DDPv phase, ReO$_2$ and the nuclear and magnetic structures of M$_{0.67}$Mn$_{0.33}$O. The main magnetic peaks are indexed on the top panel and the perovskite-superstructure peaks evidencing the A- and B-site cation orders are identified at the bottom. The main magnetic peak of M$_{0.67}$Mn$_{0.33}$O is marked *.

suggesting that high pressure stabilises a rocksalt-related M$_2$MnO$_3$ phase, but possible long range cation ordering was not detected in this study. Table 1 summarizes the refined DDPv structures of the CaMnMReO$_6$ (M = Co, Ni) compounds.

The varied neutron scattering lengths for the metals in these compounds (4.70, −3.73, 2.49, 10.3, 9.2 fm for Ca, Mn, Co,

Table 1 Sites showing Wyckoff labels, atomic coordinates, occupancies and BVS values resulting from the Rietveld fits of the room temperature NPD patterns of CaMnCoReO$_6$ (upper lines) and CaMnNiReO$_6$ (lower lines). The space group is $P4_2/n$ and cell parameters are a = 7.666(1) and 7.6868(4) Å and c = 7.6899(4) and 7.693(1) Å respectively. B_{iso} values, constrained for cations and oxygen sites, are 0.2(1) and 1.0(1) Å^2 for M = Co and 0.8(1) and 1.7(1) Å^2 for M = Ni respectively. Residuals; R_p = 2.24%, R_{wp} = 2.08%, R_f = 5.63%, R_B = 4.69% and R_p = 2.59%, R_{wp} = 3.19%, R_f = 7.09%, R_B = 5.28% respectively

Site	x	y	z	Mn/M occ	BVS
A′ (2a)	0.75	0.75	0.75	0.692/0.308(1)	1.9
				0.892/0.108(1)	1.9
A″ (2b)	0.25	0.25	0.75	0.612/0.388(1)	1.7
				0.788/0.212(1)	1.6
Ca (4e)	0.25	0.75	0.779(1)		2.0
			0.783(1)		
B (4c)	0	0.5	0.5	0.040/0.960(1)	2.0
				0.366/0.634(1)	1.7
Re (4d)	0	0	0.5		5.9
O1 (8g)	−0.055(2)	0.556(2)	0.239(1)		
	−0.049(1)	0.559(2)	0.24(1)		
O2 (8g)	−0.237(2)	−0.049(1)	0.571(1)		
	−0.240(3)	−0.049(1)	0.566(1)		
O3 (8g)	−0.263(1)	0.061(1)	−0.0298(5)		
	−0.265(2)	0.055(1)	−0.029(1)		

Ni and Re respectively)[17] provide a high degree of contrast enabling cation mixing to be investigated across the five metal sites in the AA′$_{0.5}$A″$_{0.5}$BB′O$_6$ structure. The A = Ca (ten-fold) and B′ = Re (octahedral) sites were found to be fully occupied in both materials within experimental error in the NPD refinements. CaMnCoReO$_6$ has 96% Co at the octahedral B site, but 30–40% of Co substitutes for Mn at the A′ (tetrahedral) and A″ (square planar) sites. This leads to an overall Co-rich composition CaMn$_{0.7}$Co$_{1.3}$ReO$_6$ relative to the ideal formula. CaMnNiReO$_6$ has a mix of 37% Mn and 63% Ni at the B site but with 10–20% Ni substituting at the A′ and A″ sites, leading to an overall Ni-poor composition CaMn$_{1.2}$Ni$_{0.8}$ReO$_6$. This is consistent with the higher proportion of observed M$_2$MnO$_3$ secondary phase than in the M = Co sample. Apparent lack of Ca in the products may be because this has formed amorphous phases, or crystalline products below limits of XPD detection. XPD data were fitted using the NPD structural models, and with M/Re disorder at the B-sites refined. Small antisite occupancies of 3.4(1) and 2.5(1)% for M = Co and Ni respectively show that the high charge contrast between (Mn/Co/Ni)$^{2+}$ and Re^{6+} leads to a high degree of B-site ordering.

The cation oxidation states at each atomic position have been estimated from BVS calculations,[18] as shown in Table 1, confirming that the formal charge distributions are Ca^{2+}A′$^{2+}_{0.5}$A″$^{2+}_{0.5}$B^{2+}Re^{6+}O$_6$ in both cases with A′, A″, and B sites occupied by mixtures of Mn^{2+} and Co^{2+}/Ni^{2+}. This disorder reflects the similarity of ionic radii between the divalent transition metal cations. However, no substitutions at the Ca and Re sites were found in either material.

Magnetic susceptibility and field dependent magnetization measurements are depicted in Fig. 2. CaMnCoReO$_6$ and CaMnNiReO$_6$ show ferrimagnetic behaviour below T_C = 188 and 152 K respectively. A fit of the Curie–Weiss law to the high temperature inverse susceptibilities (shown in ESI‡) results in Weiss constants θ = 188 and 151 K respectively, indicative of ferromagnetic exchange interactions for both compounds. The effective paramagnetic moments are 5.8 and 4.9 μ_B f.u.$^{-1}$ for M = Co and Ni respectively. Predicted values are 6.9 and 7.2 μ_B f.u.$^{-1}$ for the refined compositions CaMn$_{0.7}$Co$_{1.3}$ReO$_6$ and CaMn$_{1.2}$Ni$_{0.8}$ReO$_6$, assuming all cations are in high spin states. Both experimental values lie below the predicted values which most likely reflects the presence of impurity contributions to the susceptibilities. Low temperature M–H loops in Fig. 2 show that both materials have substantial saturated magnetic moments, of 4.5 and 1.8 μ_B f.u.$^{-1}$ for M = Co and Ni respectively, indicating that they have ferri- or ferro-magnetic orders at low temperature. Their coercivities are small and the M = Co hysteresis loop shows a narrowing near H = 0 indicating that competing ferro- and antiferro-magnetic exchange interactions are present.

Magnetic diffraction peaks observed in the 1.5 K NPD patterns of CaMnCoReO$_6$ and CaMnNiReO$_6$ are indexed by propagation vector [0 0 0]. Rietveld fits (R_{mag} = 5.54% and 5.83% respectively) yield the magnetic structures shown in Fig. 3. Both CaMnCoReO$_6$ and CaMnNiReO$_6$ show a simultaneous order of A and B sublattices with spins along the z axis.

Fig. 2 Magnetic susceptibilities of CaMnCoReO$_6$ (top) and CaMnNiReO$_6$ (bottom) with insets showing magnetization-field loops at 7 and 2 K respectively.

Fig. 3 Crystal and magnetic structures of CaMnCoReO$_6$ (left) and CaMnNiReO$_6$ (right) with the z-axis vertical. Orange, red, yellow, purple and blue spheres represent Ca, A′, A″, B and Re sites respectively. Polyhedra show the tetrahedral, square planar and octahedral coordination of A′, A″ and B sites, and arrows show the spin directions scaled to the refined magnitudes of the ordered moments.

All of the magnetic moments were refined independently, converging to a net ferrimagnetic arrangement of A and B sublattices

Table 2 Observed saturated magnetization at low temperatures M_{sat} and NPD refined magnetic moments for tetrahedral A′, square planar A″, and octahedral B and B′ sites, and the resulting net magnetic moment per formula unit μ, for CaMnMReO$_6$ with M = Co/Ni. All quantities are in μ_B units

M	M_{sat}	$\mu(A')$	$\mu(A'')$	$\mu(B)$	$\mu(B')$	μ
Co	4.5	2.9(1)	−1.3(1)	3.27(3)	0.3(1)	4.4
Ni	1.8	3.0(1)	1.2(2)	1.2(1)	0.2(1)	3.5

for CaMnCoReO$_6$ and their ferromagnetic alignment for CaMnNiReO$_6$, as summarised in Table 2. Other magnetic modes were not consistent with the data. See ESI‡ for further details of the magnetic symmetry analysis. An additional magnetic diffraction peak was assigned and fitted as the $(\frac{111}{222})$ peak of the M$_{0.67}$Mn$_{0.33}$O impurity phases. This peak is also observed in the 300 K pattern of CaMnNiReO$_6$. The high ordering temperature is consistent with the Néel temperatures of NiO (T_N = 523 K) and MnO (T_N = 122 K),[19] so a transition near 390 K may be interpolated for Ni$_{0.67}$Mn$_{0.33}$O. An equivalent interpolation based on T_N = 291 K for CoO predicts spin ordering around 235 K for Co$_{0.67}$Mn$_{0.33}$O, consistent with the observed appearance of magnetic neutron diffraction peaks between 300 and 1.5 K.

It is notable that all four magnetic sublattices in these two double double perovskites order ferromagnetically. The Re moments are very small, consistent with those in other Re^{6+} oxides,[16] but refine to be parallel to the other B sublattice spins whereas those in CaMnFe^{3+}Re^{5+}O$_6$ are antiparallel due to spin polarized conduction that leads to a high Curie temperature of 500 K. The T_C's below 200 K and parallel alignment of B = Co, Ni and B′ = Re spins in the CaMnMReO$_6$ (M = Co, Ni) materials indicate that they are insulating ferromagnets, although we have not yet obtained well-sintered ceramic pellets for direct conductivity measurements to confirm this. Ordered tetrahedral A′ site moments are larger than those at square planar A″ sites in both materials, reflecting the greater degree of cation disorder at the latter sites. B site moments are relatively large (3.3 μ_B) for the M = Co material which has almost no cation disorder at this site, whereas substantial Mn/Ni mixing leads to a much smaller ordered moment of 1.2 μ_B for M = Ni. The reduction of the site moments compared to ideal $2S$ values reflects magnetic disorder resulting from a complex mix of antiferro- and ferro-magnetic exchange interactions between the different sites and cation d^n configurations. This may be sensitive to the precise compositions of the studied samples, both of which are off-stoichiometric as noted above.

CaMnCoReO$_6$ is a ferrimagnet overall as the ferromagnetic A″ sublattice spins are antiparallel to those of the A′, B and B′ sublattices. The net moment of 4.4 μ_B for M = Co predicted from the NPD results is in good agreement with the observed net magnetization from the hysteresis loop (4.5 μ_B at 7 K). The refined spin structure of CaMnNiReO$_6$ is remarkable as all four ferromagnetic sublattices are parallel so this material is a rare example of a ferromagnetic (and likely insulating) oxide. The observed magnetization is below the predicted value from the

refined NPD moments, most likely reflecting the presence of the antiferromagnetic $Ni_{0.67}Mn_{0.33}O$ impurity phase. Ferrimagnetism could also account for the smaller saturated moment, but attempts to refine such models against the neutron data always resulted in the ferromagnetic spin structure shown.

In conclusion, two new members of the double double perovskite family, of ideal compositions $CaMnCoReO_6$ and $CaMnNiReO_6$, have been synthesized under high pressure and high temperature conditions. They retain the cation ordering pattern of $CaMnFeReO_6$, but with more substantial Mn/M cation mixing across three of the five available cation sites leading to non-stoichiometric $CaMn_{0.7}Co_{1.3}ReO_6$ and $CaMn_{1.2}Ni_{0.8}ReO_6$ compositions. Ferromagnetic ordering within all of their spin sublattices occurs at a single magnetic transition, unlike previous studied M = Mn and Fe analogues where two transitions were observed. $CaMnCoReO_6$ orders ferrimagnetically below $T_C = 188$ K with a relatively large saturated magnetization of 4.5 μ_B. $CaMnNiReO_6$ is a remarkable example of a ferromagnetic oxide with four distinct spin sublattices all collinearly ordered below $T_C = 152$ K.

Conflicts of interest

There are no conflicts to declare.

Notes and references

1 H. D. Megaw, *Proc. Phys. Soc.*, 1946, **58**, 326.
2 C. J. Howard and H. T. Stokes, *Acta Crystallogr., Sect. B: Struct. Sci.*, 1998, **54**, 782–789.
3 C. J. Howard, B. J. Kennedy and P. M. Woodward, *Acta Crystallogr., Sect. B: Struct. Sci.*, 2003, **59**, 463–471.
4 M. Anderson, K. Greenwood, G. Taylor and K. Poeppelmeier, *Prog. Solid State Chem.*, 1993, **22**, 197–233.
5 R. H. Mitchell, *Perovskites: Modern and ancient*, Almaz Press, Ontario, Canada, 2002.
6 G. King and P. M. Woodward, *J. Mater. Chem.*, 2010, **20**, 5785–5797.
7 K. Lienenweber and J. Parise, *J. Solid State Chem.*, 1995, **114**, 277–281.
8 A. Aimi, D. Mori, K. Hiraki, T. Takahashi, Y. J. Shan, Y. Shirako, J. Zhou and Y. Inaguma, *Chem. Mater.*, 2014, **26**, 2601–2608.
9 S. Vasala and M. Karppinen, *Prog. Solid State Chem.*, 2015, **43**, 1–36.
10 M. C. Knapp and P. M. Woodward, *J. Solid State Chem.*, 2006, **179**, 1076–1085.
11 G. King, S. Thimmaiah, A. Dwivedi and P. M. Woodward, *Chem. Mater.*, 2007, **19**, 6451–6458.
12 P. Zuo, H. Klein, C. Darie and C. V. Colin, *J. Magn. Magn. Mater.*, 2018, **485**, 48–51.
13 C. De and A. Sundaresan, *Phys. Rev. B*, 2018, **97**, 214418.
14 E. Solana-Madruga, A. M. Arévalo-López, A. J. Dos santos-García, E. Urones-Garrote, D. Avila-Brande, R. Sáez-Puche and J. P. Attfield, *Angew. Chem., Int. Ed.*, 2016, **55**, 9340–9344.
15 E. Solana-Madruga, A. M. Arévalo-López, A. J. Dos santos-García, C. Ritter, C. Cascales, R. Sáez-Puche and J. P. Attfield, *Phys. Rev. B*, 2018, **97**, 134408.
16 G. M. McNally, A. M. Arévalo-López, P. Kearins, F. Orlandi, P. Manuel and J. P. Attfield, *Chem. Mater.*, 2017, **29**, 8870–8874.
17 V. F. Sears, *Neutron News*, 1992, **3**, 26–37.
18 J. P. Attfield, *Solid State Sci.*, 2006, **8**, 861–867.
19 W. L. Roth, *Phys. Rev.*, 1958, **110**, 1333–1341.